Int. J. Heat Mass Transfer. Vol. 27, No. 8, pp. 1205–1218, 1984
Printed in Great Britain

0017-9310/84 $3.00 + 0.00
Pergamon Press Ltd.

THERMOGRAVITATIONAL AND THERMOCAPILLARY FLOWS IN A HORIZONTAL LIQUID LAYER UNDER THE CONDITIONS OF A HORIZONTAL TEMPERATURE GRADIENT

A. G. KIRDYASHKIN*

Institute of Thermophysics of the Siberian Branch of the U.S.S.R. Academy of Sciences, 630090, Novosibirsk, U.S.S.R.

(*Received* 30 *November* 1982)

Abstract—This paper presents an experimental investigation of the thermal and dynamic structures of thermogravitational flows in a horizontal layer heated from the side and having two rigid boundaries. The upper surface of the layer is free and the lower is rigid and adiabatic. This provides a situation for a simultaneous occurrence of the thermogravitational and thermocapillary forces. The boundaries of the heat transfer regimes have been found and for each the heat transfer laws have been determined. For the regime characterized by a constant longitudinal temperature gradient (far from vertical end surfaces), the laws governing the velocity and temperature field variation depending on the heat flux have been found analytically.

NOMENCLATURE

A	horizontal temperature gradient, $\partial T/\partial x$
a	thermal diffusivity
b	temperature coefficient of surface tension, $\partial\sigma/\partial T$
c_p	heat capacity at constant pressure
g	gravity acceleration
$2l$	layer height
Ma	Marangoni number, $bl\Delta T/\rho\nu a$
Nu	Nusselt number, $\alpha l/\lambda = Q/2\lambda\Delta T$
P	pressure
Pr	Prandtl number, ν/a
Q	quantity of heat transferred in a horizontal direction (per unit of measurement over the layer width)
Ra	Rayleigh number, $\beta g\Delta T l^3/a\nu$
T	temperature
ΔT	temperature difference between horizontal upper and lower bounding adiabatic surfaces
T_l, T_{-l}	temperature of upper and lower horizontal adiabatic surfaces, respectively
ΔT_1	temperature difference between hot and cold vertical side surfaces, $T_h - T_c$
T_m	mean temperature over layer depth
u	horizontal velocity component
x_0	layer length
y, x, z	vertical and horizontal coordinate axes
z_0	layer width.

Greek symbols

β	coefficient of thermal expansion of liquid
λ_T, λ	thermal conductivities of a massif and liquid
μ, ν	dynamic and kinematic viscosity coefficients
ρ	density.

INTRODUCTION

THE FLOWS in a horizontal layer of liquid due to a horizontal temperature gradient are considered. In actual conditions, this is a plane liquid layer the horizontal dimension (x_0) of which is much larger than its height ($2l$), $x_0/2l \gg 1$ (Fig. 1). In the region of vertical end surfaces, the flow changes its direction by 180°. Due to the horizontal temperature gradient the developing flow in the field of gravitational forces is directed along the normal to the gravity force vector (in contrast to a vertical layer, $x_0/2l \ll 1$, which is heated and cooled from the side and where the flow is ascending at the hot, and descending at the cold surface).

These insufficiently known flows are observed in the earth's atmosphere and its ocean. In the earth's atmosphere, which is, on the average, stably stratified, the horizontal temperature gradients prevail from the poles to the equator, between the continents and the oceans, and the periodic in time and space horizontal gradients occur due to seasonal and diurnal variations of temperature. In the earth's ocean, the horizontal temperature gradients induce the so-called entrusive jet flows. According to the geologistic investigations, the entrusions of different compositions are observed in the earth's crust; their origin can be explained by the

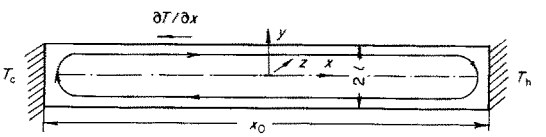

FIG. 1. Schematic diagram of liquid flow in a horizontal layer heated on one side.

* Permanent address: Institute of Geology and Geophysics of the Siberian Branch of the Academy of Sciences of the U.S.S.R., 630090, Novosibirsk, U.S.S.R.

existence of horizontal density gradients. The flows originating under the action of horizontal temperature gradients can be observed in shallow water pools used for waste heat removal.

The interest in the kind of flow considered has also arisen in connection with the choice of the optimum conditions for obtaining high-quality materials and crystals; for example, in the technology of single crystal production such a kind of pool is called a 'boat': melting or dissolution of the substance occurs on one vertical end face of the boat and a crystal is grown from this substance on the other.

In the case of large horizontal dimensions and small horizontal temperature gradients, $\partial T/\partial x$, the flow far from the vertical end faces can be expected to be plane-parallel.

Theoretically the problem of thermogravitational and thermocapillary convection in a horizontal infinite liquid layer was investigated in ref. [1]. In the absence of a temperature drop between horizontal surfaces, the solutions for the temperature and velocity distribution over the layer depth have been obtained and the conditions of heat transfer on the horizontal surfaces, under which the temperature gradient is constant throughout the layer, have been found. Close to the horizontal heat transfer surfaces, the regions of unstable stratification are observed and the temperature gradient in proximity to the surfaces is negative. The stability of this type of flow was investigated in the linear approximation in refs. [2–5], and the trends in the development of finite-amplitude spatial perturbations in the vicinity of the stability loss point were considered in ref. [6].

At present, this type of flow [1] has not been realized experimentally owing to the complex nature of the boundary conditions. It is probable that the boundary conditions may comply approximately if the horizontal layer is surrounded by a solid massif (two vertical side end faces are insulated). In a solid massif the horizontal gradient, $A = \partial T/\partial x = \text{const.}$, and the horizontal specific heat flux is much larger than the vertical one directed to the liquid near the lower horizontal surface and from it to the massif at the upper horizontal surface. As it follows from ref. [1], in this case the following condition should be fulfilled: $\lambda_T/\lambda \gg \beta g A l^4/45 a\nu$, where λ_T and λ are the thermal conductivity coefficients of the massif and liquid, respectively. The degree of the above inequality fulfilment and the dimension of the horizontal layer, $x_0/2l$, will depend on the degree of fulfilment of the following conditions: (a) the absence of a temperature drop between the horizontal surfaces; (b) $A = \text{const.}$ throughout the layer far from the vertical end faces.

The stability of flows under the above boundary conditions [1] and in the case of thermal insulation of horizontal bounding surfaces have been studied in the linear approximation in ref. [7].

The most simple boundary conditions realizable in the laboratory are the conditions of thermal insulation of horizontal bounding surfaces, $(\partial T/\partial y)_{y=\pm l} = 0$, when the source and the sink of the heat are located on the opposite vertical end faces.

The results of experimental investigations in a layer with rigid adiabatic bounding horizontal surfaces with a constant temperature difference between the isothermal vertical end faces are presented in refs. [8, 9]. The temperature and velocity profiles measured throughout the layer have shown that in the main stream the flow has a plane-parallel pattern [8] and, near the bounding horizontal surfaces, a boundary-layer pattern [9].

The results of numerical experiments for a horizontal layer, $x_0/2l \gg 1$, heated from the side with horizontal adiabatic surfaces are presented in refs. [10–12]. In refs. [13, 14], the rate of heat transfer through a horizontal layer with adiabatic horizontal surfaces and with isothermal vertical differently heated end faces is determined by joining the solution for the main stream with the approximate solutions for the flow near a vertical end face. The investigations described in ref. [15] are concerned with the flow near a vertical surface and its interaction with a horizontal flow in the layer core.

In the present work experimental investigations of the velocity and temperature profiles in a horizontal layer of liquid, $7 \leqslant x_0/2l \leqslant 90$, with free and rigid insulated surfaces are carried out under the conditions of thermocapillary and thermogravitational convection. The conditions of the heat conduction and boundary layer regimes and of the convective heat transfer regime under the conditions of a plane-parallel flow have been found, with the heat transfer law being determined for each of these. For the regimes characterized by a constant temperature gradient, A, the laws governing a change in the velocity and temperature fields depending on the heat flux transported through the layer have been found analytically and compared with the experimental results available.

EXPERIMENTAL FACILITY

Experimental investigations were carried out on a set-up consisting of a rectangular bath (1) measuring $150 \times 150 \times 900$ mm (Fig. 2). For the purpose of thermal insulation the side walls of the bath were constructed from double Perspex plates ($10 \times 150 \times 920$ mm) air-spaced for the front transparent wall and with a 15 mm thick polyurethane foam insert for the rear wall. The bottom of the bath consisted of a 3 mm thick Perspex plate (2) which rests on a $90 \times 170 \times 1000$ mm

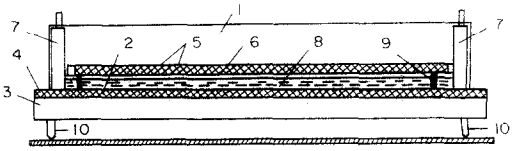

FIG. 2. Schematic diagram of experimental set-up.

foam plastic support (3) covered with a polyurethane foam plate (4) measuring $15 \times 170 \times 1000$ mm.

The top horizontal plate was made of two Perspex plates (5) ($3 \times 145 \times 810$ mm) so as to form a $15 \times 125 \times 790$ mm cavity filled with polyurethane foam (6). The horizontal insulating plates $x_0 = 412$ and 810 mm long have transparent slits ($\delta = 5$ mm) along the whole length at distances $z = 45$ and 75 mm from the front end face.

On the vertical end faces of the bath, heat exchangers (7), made of a $10 \times 148 \times 148$ mm brass plate and a Perspex plate in such a way as to form a cavity measuring $20 \times 130 \times 130$ mm, were mounted. The constancy of temperature of the heat-transfer surfaces was ensured by temperature-controlled water circulation in the cavity of the heat exchanger. Thermostats capable of keeping the temperature constant to within $\pm$ 0.03°C were used. The temperature of each of the heat transfer surfaces was measured with nichrome–constantan thermocouples made of 0.1 mm diameter wires. The thermocouples were inserted into 0.8 mm diameter cylinders and could be mounted into 1 mm diameter holes in the end faces drilled at different heights 0.5 mm away from the heat transfer surface. The liquid (water, ethyl alcohol 96%) layer (8) thickness was set with the aid of 3 mm thick gauge plates (9) on which the top horizontal plate was mounted. In case of two rigid bounding surfaces, the liquid contacts with the top plate. The free surface was created by filling the bath up to the required height short of the top plate (5). The distance between the free liquid surface and the top insulated horizontal plate was 5–7 mm. The horizontal position of the bath was adjusted by set screws (10).

The temperature in the liquid layer was measured with a thermocouple probe consisting of two nichrome–constantan thermocouples made of 0.1 mm diameter wires. The probe was introduced through a 5 mm slit between the rear wall of the bath and the end face of the top horizontal plate (5). The thermocouples were placed one above the other making it possible to bring one of these respectively right up to the top and bottom walls. The thermocouple could move vertically (y) and horizontally (x) and, by turning the probe, also along z. The probe displacement in the vertical direction was controlled by a KM-8 cathetometer accurate to within 0.01 mm and also by using a 0.05 mm scale fixed on the traverse gear. The e.m.f. of the thermocouples was measured with a digital voltammeter $\Phi - 30$.

The liquid flow velocity in the layer was measured by means of flow visualization implemented by using aluminium particles kept in the liquid throughout the whole experiment lasting 9–10 h. The layer with the particles was transparent over its whole width (z_0). The largest value of the horizontal velocity component did not exceed 2.5 mm s^{-1}. Therefore, the velocity was determined from the time required for a particle to traverse the distance fixed on the telescope graticule of the KM-8 cathetometer. After the bath was filled up with liquid and the top horizontal plate (5) was set

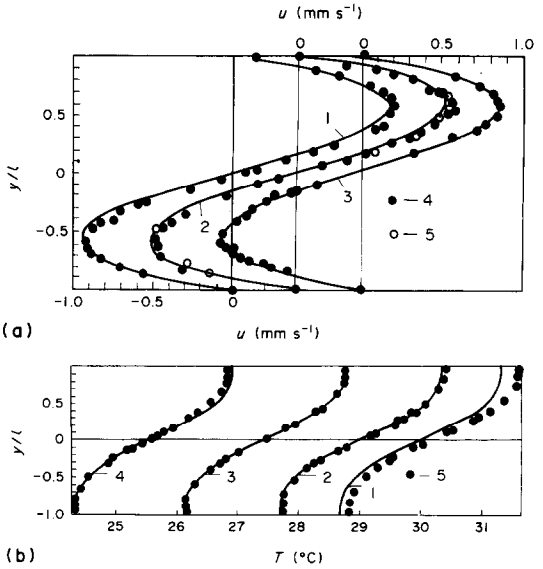

FIG. 3. Profiles of velocity (a) and temperature (b) in a horizontal layer of water of thickness $2l = 14.45$ mm, $Ra = 2.2 \times 10^4$; $T_h = 26.5$°C; $T_c = 18.5$°C; $x_0 = 810$ mm. (a) 1–3, calculated from equation (16) $T_m = 29.1$, 27.5, 25.6°C for $x = 243$, 378, 565 mm, respectively; 4, experimental points at $x = 243$, 378, 565 mm corresponding to Curves 1–3, $z = 45$ mm; 5, experimental points at $x = 378$ mm and $z = 75$ mm. (b) Calculation by equations (17) and (18): 1, $x = 165$ mm; 2, $x = 250$ mm; 3, $x = 385$ mm; 4, $x = 545$ mm; 5, experimental points corresponding to Curves 1–4.

(Fig. 2), the gaps between the bath and the plate were insulated against ambient heat and moisture, so that no marked volumetric evaporation of the test liquid was noticed during the entire experiment. The experiments were carried out with liquid layers $x_0/2l = 7$–90. In Fig. 3(a) a velocity profile is given for $x = 378$ mm measured at different distances from the front side end face ($z = 45$ mm, points 4; and 75 mm, points 5); x is the distance from the hot plate. It is seen that at a distance of 45 mm the vertical end face does not influence the velocity profile. The velocity measurements were carried out at $z = 45$ mm for the layer of thickness $2l < 15$ mm. Figures 3(a) and 4(a) present the velocity profiles in the layer of water and ethyl alcohol, respectively, when the upper liquid surface layer is free (does not contact with the top insulating plate). As is seen from Fig. 3(a), the free surface of distilled water is stagnant ($u_{y=1} = 0$), i.e. behaves as a rigid surface, which is due to the presence of surfactants in it.

The experimental investigations have shown that in thin horizontal layers of liquid, the flow has largely a plane-parallel pattern [Figs. 3(a) and 4(a)]. This agrees with the results of ref. [8]. Figures 3(b) and 4(b) present the temperature profiles over the layer depth for different distances x from the hot vertical plate. The upper and lower horizontal surfaces are good insulators. Here, the condition $(\partial T/\partial y)_{y=\pm 1} = 0$ is well fulfilled, i.e. the heat flux along the normal to the surface is absent. A change in the temperature on the insulated horizontal surfaces at a sufficient distance from the hot and cold vertical heat exchangers is linear with respect

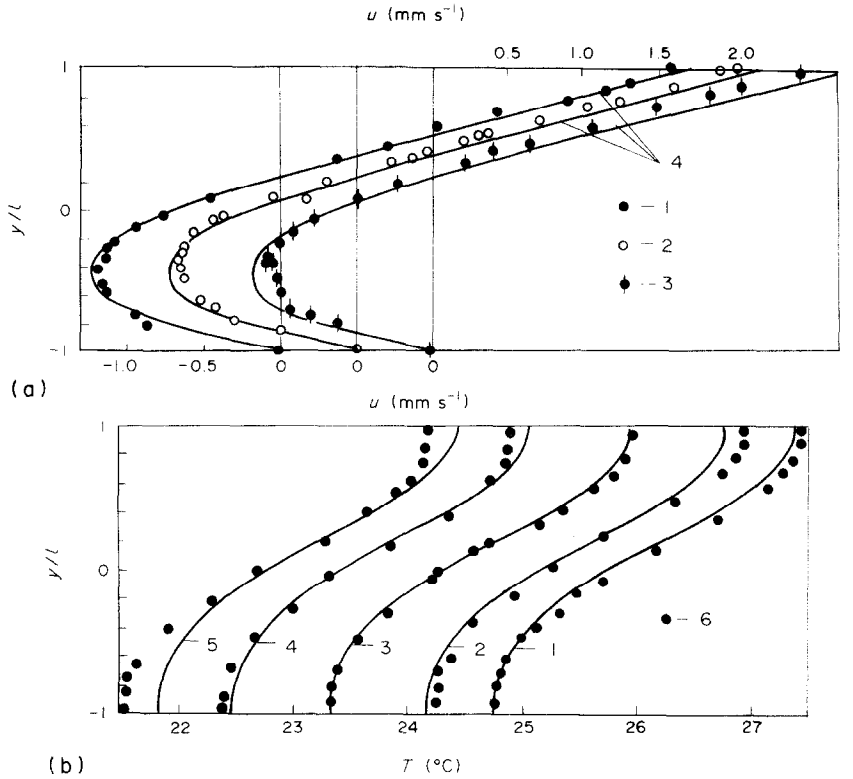

FIG. 4. The profiles of velocity (a) and temperature (b) in a horizontal layer of ethyl alcohol with the free upper boundary, $2l = 9.4$ mm, $Ma = -1.1 \times 10^4$, $Ra = 2.2 \times 10^4$, $k = -0.5$, $T_h = 32.5°C$, $T_c = 18.1°C$, $x_0 = 412$ mm. (a) Experimental values: 1, $x = 120$ mm; 2, $x = 221$ mm; 3, $x = 300$ mm; 4, from equation (30). (b) From equations (18) and (31): 1, $x = 46$ mm; 2, $x = 110$ mm; 3, $x = 200$ mm; 4, $x = 300$ mm; 5, $x = 375$ mm; 6, experimental points corresponding to Curves 1–5.

to x [Figs. 3(b) and 4(b)]. The temperature profiles over the boundary layer depth shift equidistantly on moving away from the heat transfer surface. Over a greater portion of the layer length and over its whole depth ($2l$), there is a constant longitudinal temperature gradient $A = \partial T/\partial x = \text{const.}$; the temperature drop between the upper horizontal surface (T_l) and lower one (T_{-l}) is also constant, $\Delta T = T_l - T_{-l} = \text{const}$.

In the central part of a thin horizontal layer, heated and cooled from two vertical end faces, the flow is plane-parallel with a constant temperature drop between the insulating horizontal surfaces and with a constant longitudinal temperature gradient on them and in the layer. This problem is similar to that considered in ref. [1], but with different boundary conditions. Therefore, its solution will be considered in more detail.

THEORY

(1) An infinite, along x, horizontal layer is considered. The heat sources are removed *ad infinitum*. The coordinate origin is in the centre of the layer, the coordinates of the horizontal boundaries are $y = \pm l$. The flow has a plane-parallel pattern (Fig. 5).

$$u_x = u(y); \quad u_y = 0; \quad u_z = 0. \tag{1}$$

The heat flux through the horizontal surfaces is absent and the temperature drop between them is constant

$$\left(\frac{\partial T}{\partial y}\right)_{y=\pm l} = 0, \quad \Delta T = \text{const}. \tag{2}$$

In this case the equations of the thermogravitational convection are of the form

$$\frac{1}{\rho}\frac{\partial P}{\partial y} = \beta g T; \quad \frac{1}{\rho}\frac{\partial P}{\partial x} = \nu\frac{\partial^2 u}{\partial y^2}; \tag{3}$$

$$u\frac{\partial T}{\partial x} = a\left(\frac{\partial^2 T}{\partial y^2} + \frac{\partial^2 T}{\partial x^2}\right). \tag{4}$$

The condition for the flow to be closed is

$$\int_{-l}^{l} u\,dy = 0. \tag{5}$$

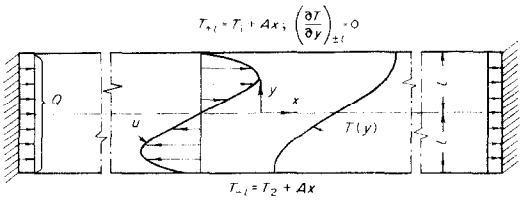

FIG. 5. Schematic representation of the velocity and temperature profiles in a layer with rigid bounding surfaces.

Excluding the pressure from equations (3) yields

$$\nu\frac{\partial^3 u}{\partial y^3}=\beta g\frac{\partial T}{\partial x}. \tag{6}$$

The LHS of equation (5) depends only on y. This is possible only when $\partial T/\partial x=\text{const.}$, i.e. on the horizontal surfaces

$$T_l=T_1+Ax;\quad T_{-l}=T_2+Ax. \tag{7}$$

The solution for the temperature is

$$T=T(y)+Ax. \tag{8}$$

Now substitute equation (8) into equations (3) and (4) and present them in dimensionless form as

$$\frac{\partial^3 u}{\partial y^3}=A; \tag{9}$$

$$\frac{\partial^2\theta}{\partial y^2}=A\,Ra\,u, \tag{10}$$

where l is the length scale, ΔT is the temperature scale, $Ra(a/l)$ is the velocity scale; $Ra=\beta g\Delta T l^3/a\nu$ is the Rayleigh number; $\theta=[T(y)-T_2]/\Delta T$.

Integration of equation (9) over y yields

$$A^{-1}u=\frac{y^3}{3!}+c_1\frac{y^2}{2!}+c_2y+c_3. \tag{11}$$

Substitution of equation (11) into equation (10) and integration over y gives

$$(A^2\,Ra)^{-1}\theta=\frac{y^5}{5!}+c_1\frac{y^4}{4!}+c_2\frac{y^3}{3!}+c_3\frac{y^2}{2!}+c_4y+c_5. \tag{12}$$

The boundary conditions for the case of thermogravitational convection with two rigid horizontal surfaces are

$$u=0\quad\text{at}\quad y=\pm1; \tag{13}$$

$$\theta=1,\quad\frac{\partial\theta}{\partial y}=0\quad\text{at}\quad y=1,\quad\theta=0,$$

$$\frac{\partial\theta}{\partial y}=0\quad\text{at}\quad y=-1. \tag{14}$$

Conditions (5), (13) and (14) determine the constants of integration in equations (11) and (12) and also determine A. Simple calculations give

$$A=\pm\left(\frac{45}{2Ra}\right)^{1/2}. \tag{15}$$

Here, the sign is determined by the direction of the coordinate x. When x is directed from the hot wall, $A=-(45/2Ra)^{1/2}$.

The velocity and temperature of the liquid are determined from

$$u=\left(\frac{5}{8Ra}\right)^{1/2}(y-y^3); \tag{16}$$

$$\theta=\frac{1}{16}(3y^5-10y^3+15y+8). \tag{17}$$

Substitution of equation (17) into equation (8) yields

$$(T-T_2)/\Delta T=\theta+Ax. \tag{18}$$

Since there is no heat flux through the bounding horizontal surfaces $(\partial T/\partial y)_{y=\pm l}=0$, then the quantity of heat transported in the horizontal direction per unit length across the layer width is determined from

$$Q=\int_{-l}^{l}\left(\rho c_p uT-\lambda\frac{\partial T}{\partial x}\right)\mathrm{d}y, \tag{19}$$

where c_p is the heat capacity at constant pressure. Equations (19) and (15)–(18) determine the quantity of heat transferred through the layer per unit width as

$$Q=\lambda\Delta T\left[\left(\frac{90}{Ra}\right)^{1/2}+\left(\frac{10Ra}{441}\right)^{1/2}\right]. \tag{20}$$

The dimensionless heat transfer coefficient ($Nu=\alpha l/\lambda=Q/2\lambda\Delta T$) is found from the equation

$$Nu=\left(\frac{45}{2Ra}\right)^{1/2}+\left(\frac{5Ra}{882}\right)^{1/2}. \tag{21}$$

The first term in these relations shows the quantity of heat transported by heat conduction; the second term is the quantity of heat contributed by convection. At $Ra\simeq63$, the quantities of heat transferred by conduction and convection are the same. At $Ra\ll63$, the heat is mainly transferred by conduction, and at $Ra\gg63$, by convection.

Equation (20) establishes an unambiguous dependence between the quantity of heat transported and the temperature drop between the insulated horizontal surfaces, and, for example at $Ra\ll63$

$$\Delta T=\frac{\beta g l^3}{90a\nu}\left(\frac{Q}{\lambda}\right)^2;\quad Ra=\frac{1}{90}\left(\frac{\beta g l^3 Q}{a\nu\lambda}\right)^2; \tag{22}$$

at $Ra\gg63$

$$\Delta T=(44.1)^{1/3}\left(\frac{Q}{\lambda}\right)^{2/3}\left(\frac{a\nu}{\beta g l^3}\right)^{1/3};$$

$$Ra=(44.1)^{1/3}\left(\frac{\beta g l^3 Q}{a\nu\lambda}\right)^{2/3}. \tag{23}$$

In the case of the developed flow far from the end faces in a layer with insulated horizontal surfaces, the initial parameters of the problem are the heat flux in the horizontal layer (or the temperature drop on the adiabatic walls) and the layer height. The determining criterion of the process is the Rayleigh number based on ΔT or Q and on l. Here, it is not necessary to know the mode of heat transfer on vertical end faces—conduction, boundary layer or transition regimes.

However, if the temperature drop is set on the vertical end faces, $\Delta T_1=T_h-T_c$, then the determining parameters of the problem will be: $Ra_1=\beta g\Delta T_1 l^3/a\nu$; $Pr=\nu/a$, and the relative layer dimension will be $x_0/2l$. In this case it is necessary to solve a general problem

including also the end regions where the flow changes its direction by 180°.

For the heat conduction regime, at which $\partial T/\partial x = \text{const.}$, one can find, throughout the whole layer (including the end regions), the dependence between the temperature drop on the vertical heat transfer surfaces and the temperature drop on the adiabatic horizontal surfaces.

The temperature gradient in the layer is determined from equation (15) as $\partial T/\partial x = (45/2Ra)^{1/2}(\Delta T/l)$; in the heat conduction regime $\partial T/\partial x = \Delta T_1/x_0$. By equating the RHSs of these expressions, one obtains

$$\frac{\Delta T}{\Delta T_1} = \frac{2}{45}\left(\frac{l}{x_0}\right)^2 Ra_1; \quad \frac{\Delta T}{\Delta T_1} = \left(\frac{2Ra}{45}\right)^{1/2}\left(\frac{l}{x_0}\right). \tag{24}$$

For the other heat transfer modes on the vertical walls (the transitional—from the heat conduction to the boundary layer—regime on the vertical end face and the boundary layer regime), the dependence between ΔT and ΔT_1 can be found either by the methods of numerical experiment, or by joining the solutions for the plane-parallel flow in the core of the horizontal layer with the approximate solutions for the flow near the vertical end face [10, 11]. The latter method is an approximate one and requires experimental verification.

(2) Consider the case when the upper surface is free and there are no surfactants in the liquid which can alter the surface tension or lead to the strengthening of the free surface to such an extent that it will become completely stagnant (Fig. 6). Here, the friction forces can be accompanied by the thermocapillary forces caused by a temperature-induced change in the surface tension.

The equilibrium condition in the problem considered is written in the form [1]

$$\rho\nu\left(\frac{\partial u}{\partial y}\right)_{y=l} = \frac{\partial\sigma}{\partial T}\cdot\frac{\partial T}{\partial x}. \tag{25}$$

This can be represented in dimensionless form as

$$\left(\frac{\partial u}{\partial y}\right)_{y=1} = A\frac{Ma}{Ra}, \tag{26}$$

where $Ma = bl\Delta T/\rho\nu a$ is the Marangoni number; $b = \partial\sigma/\partial T$ and is the negative value for the majority of liquids.

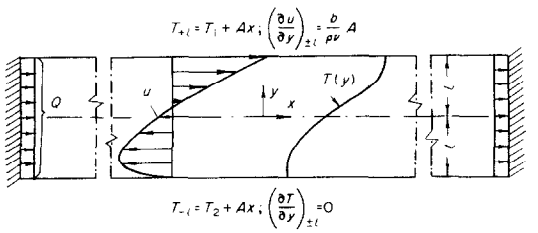

FIG. 6. Schematic representation of the velocity and temperature profiles in a layer with the upper boundary being free.

On the lower boundary

$$u = 0 \quad \text{at} \quad y = -1. \tag{27}$$

The boundary conditions for the temperature are

$$\theta = 1, \quad \frac{\partial\theta}{\partial y} = 0 \quad \text{at} \quad y = 1; \qquad \theta = 0, \quad \frac{\partial\theta}{\partial y} = 0 \quad \text{at} \quad y = -1. \tag{28}$$

After simple calculations, from conditions (5) and (26)–(28) it is possible to determine the constants of integration in equations (11) and (12) and the value of A

$$A = \pm\left(\frac{30}{(3-5k)Ra}\right)^{1/2}, \tag{29}$$

where $k = Ma/Ra = b/\beta\rho gl^2$; the minus sign is for the case when x is directed from the hot surface.

The relationships for the velocity and temperature profiles have the form

$$u = -[30/(3-5k)Ra]^{1/2}\left[\frac{y^3}{6} + \frac{3k-1}{8}y^2 + \frac{k-1}{4}y - \frac{3k-1}{24}\right], \tag{30}$$

$$\theta = \frac{5}{12-20k}\left[\frac{y^5}{5} + \frac{3k-1}{4}y^4 + (k-1)y^3 + \frac{1-3k}{2}y^2 + (2-3k)y - \frac{5k}{4} + \frac{19}{20}\right]. \tag{31}$$

The temperature distribution in the layer is determined from equations (18) and (31).

Using equations (19) and (29)–(31), it is possible to determine the quantity of heat transported by a $2l$ thick layer per unit width and the Nusselt number ($Nu = \alpha l/\lambda$; $\alpha = q/\Delta T$; $q = Q/2l$)

$$Nu = \frac{Q}{2\lambda\Delta T} = \left[\frac{30}{(3-5k)Ra}\right]^{1/2} + \frac{1}{(3-5k)} \times \left(\frac{96Ra}{5}\right)^{1/2}\left(\frac{8K^2}{35} - \frac{4K}{15} + \frac{76}{945}\right). \tag{32}$$

Here, the first term represents the quantity of heat transported by heat conduction; the second term, by convection. The relationship expresses the dependence between the quantity of heat transmitted and the temperature drop established on horizontal adiabatic walls.

When the temperature coefficient of surface tension on a free surface $b = 0$, then A, velocity, temperature, and heat flux can be found from relations (29)–(32), provided $k = 0$.

Under the conditions of thermocapillary convection ($g = 0$, $Ra = 0$), a plane liquid layer with one free boundary may be realized if one plane bounding surface is wetted, while the other and all the side end surfaces are not wetted with liquid, and the volume is moderately filled with liquid. Then in the case of heating and cooling of two opposite end surfaces, with the

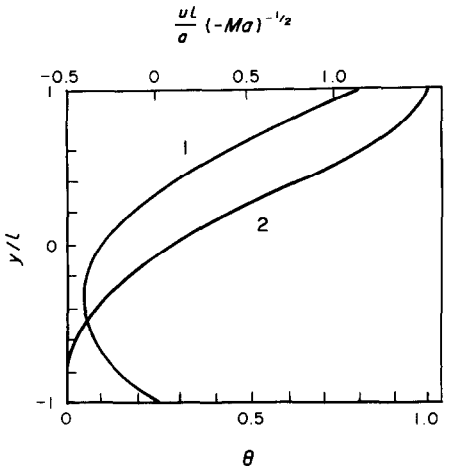

FIG. 7. The velocity profiles, 1 [from equation (34)], and temperature profiles, 2 [from equation (35)], under the conditions of thermocapillary convection and $g = 0$.

remaining surfaces being insulated, the temperature and velocity profiles and also A and Nu in the plane-parallel flow regime over the central portion of a thin liquid layer are determined from equations (29)–(32) at $g = 0$, $Ra = 0$

$$A = \pm[6/(-Ma)]^{1/2}; \tag{33}$$

$$(-Ma)^{-1/2}\frac{ul}{a} = \frac{6^{1/2}}{8}(3y^2+2y-1); \tag{34}$$

$$\theta = -0.25\left(\frac{3y^4}{4}+y^3-\frac{3y^2}{2}-3y-\frac{5}{4}\right); \tag{35}$$

$$Nu = \left(\frac{6}{-Ma}\right)^{1/2}+\frac{32}{875}(-6Ma)^{1/2}. \tag{36}$$

The velocity and temperature profiles are presented in Fig. 7.

EXPERIMENTAL RESULTS AND THEIR ANALYSIS

Figures 3(a) and (b) compare experimental velocity and temperature profiles with solutions (16)–(18) obtained for a layer of water. The free surface behaves as a rigid one. The physical constants of liquids (water, ethyl alcohol 96%) were determined from T_m according to ref. [17]. It should be noted that at the available values of the temperature gradient along the layer length A the differences occur between the predicted maximum velocities, when in each section x a corresponding value of temperature, averaged over the layer depth, is taken [Fig. 3(b)]. The same tendency in the behaviour of u is observed experimentally. Figure 3(a) presents the velocity profiles which were determined from T_m at the corresponding value of x by equation (16). There is a good coincidence between theoretical and experimental velocity values over the depth of the layer and along the greater part of its length. Some differences between the experimental values of temperature and those predicted by equations

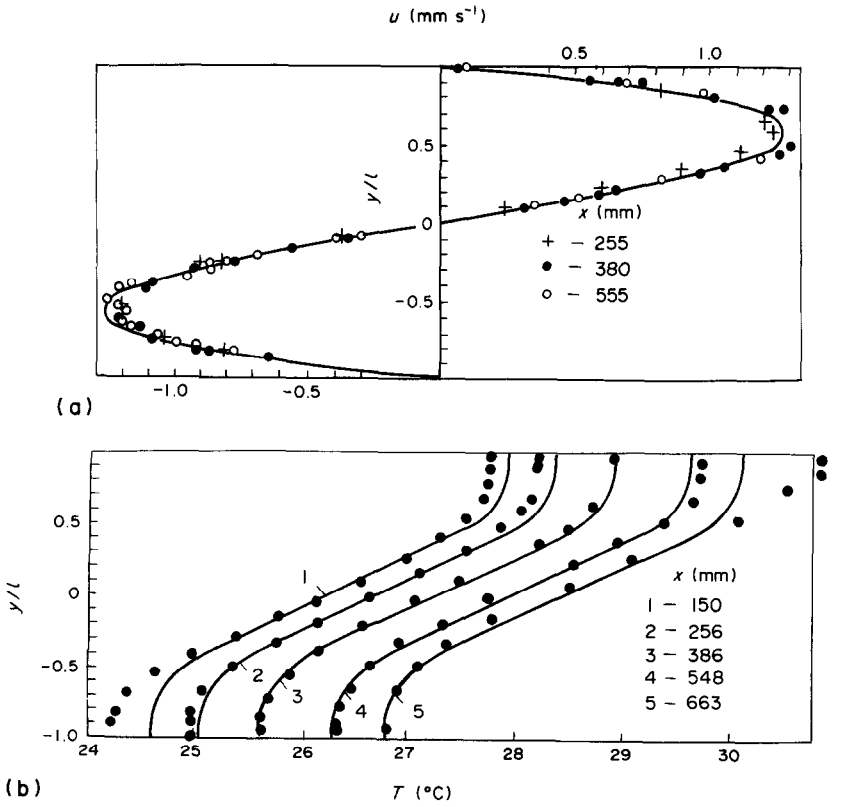

FIG. 8. Profiles of velocity (a) and temperature (b) over the layer depth $2l = 22.7$ mm, $x_0 = 810$ mm, $Ra = 1.07 \times 10^5$, $Pr = 5.7$.

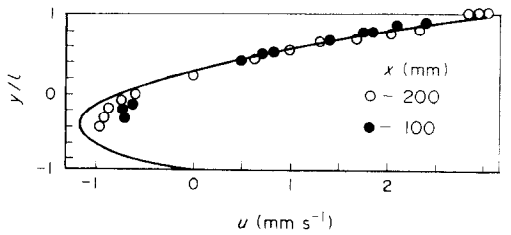

FIG. 9. The velocity profile in an ethyl alcohol layer with a free boundary: $2l = 4.62$ mm, $Ma = -4.37 \times 10^3$, $Ra = 2.3 \times 10^5$, $k = -1.9$; $T_h = 40.7°C$, $T_c = 22.5°C$; $T_m = 30°C$, $x_0 = 412$ mm; the line is calculated by equation (30).

(17) and (18) are observed at $x/2l = 11$. The calculation by equations (17) and (18), presented in Fig. 3(b) was made at the base temperature $T_{-l} = 26.15°C$ for $x = 385$ mm. The correspondence between the experiment and prediction is fair over the greater portion of the layer length.

In Figs. 8(a) and (b) the experimental values of velocity and temperature are presented as points. The curves show calculation by equations (16)–(18). There is a satisfactory agreement between the experimental and theoretical velocity values. The temperature profiles become somewhat different from theoretical ones closer to the end faces [Fig. 8(b)]. The calculation by equations (17) and (18) was made at the base temperature $T_{-l} = 25.6°C$ for $x = 424$ mm.

Figures 4(a) and (b) and 9 compare the velocity and temperature profiles measured experimentally with those calculated by equations (30), (31) and (18) for the layers of ethyl alcohol with the upper boundary free. When calculating the temperature profiles in the layer $2l = 9.4$ mm [Fig. 4(b)], it was assumed that $T_{-l} = 23.35°C$ for $x = 200$ mm. In the temperature range studied for the 96% ethyl alcohol, $b = -9 \times 10^{-5}$ N m^{-1}°C^{-1} [17].

The comparison shows the coincidence between the experimental and theoretical velocity and temperature profiles at different ratios of thermocapillary and thermogravitational forces ($k = -0.5$ and -1.9). The

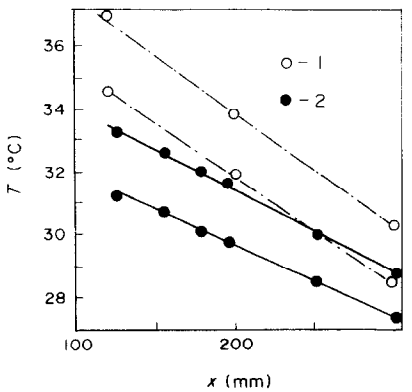

FIG. 10. The temperature of the bounding surfaces: 1, a layer of water with rigid boundaries, $2l = 8.0$ mm, $Ra = 3.7 \times 10^3$, $x_0 = 412$ mm; 2, ethyl alcohol layer with a free boundary, $2l = 4.62$ mm, $Ma = -4.37 \times 10^3$, $k = -1.9$, $x_0 = 412$ mm.

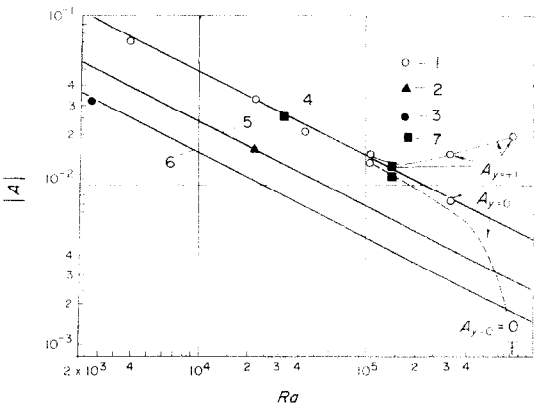

FIG. 11. The dependence of $|A|$ on Ra: 1, rigid surfaces, water, free boundary in the layer of ethyl alcohol; 2, $k = -0.5$; 3, $k = -1.9$; 4, from equation (15); 5, from equation (29) at $k = -0.5$; 6, from equation (29) at $k = -1.9$; 7, rigid surfaces for water layer from ref. [8].

temperature variation on the horizontal bounding surfaces is shown in Fig. 10. The dimensionless longitudinal temperature gradients and their comparison with the values predicted from equations (15) and (29) are presented in Fig. 11 for the respective values of Ra and k. There is a good coincidence between the experiment and theory.

For the case of two rigid adiabatic horizontal surfaces (water layer) the values of A were determined experimentally for different values of Ra (Fig. 11). At $Ra < 10^5$, there is a good coincidence between the results calculated from equation (15) and the experimental values: the temperature gradient A is constant over the entire layer depth and over the greater portion of its length excluding the end face regions. At $Ra > 1.07 \times 10^5$ and $x_0/2l = 35.6$, there is a difference between the temperature gradient at $y = 0$ and ± 1 near the bounding horizontal surfaces [Figs. 8(b) and 11]. At the centre of the layer $A_{y=0}$ is somewhat smaller than $A_{y=\pm 1}$. The same differences are observed in the experiments described in ref. [8] where the temperature profiles were calculated on horizontal surfaces and at the centre of the layer. These differences increase with an increasing Ra and at $Ra = 7.1 \times 10^5$ the temperature gradient at the cross-section $y = 0$ (in the central portion of the layer) is absent, i.e. $A_{y=0} = 0$ [Figs. 11 and 12(a) and (b)]. The temperature gradient $A_{\pm 1}$ near the bounding adiabatic horizontal surfaces varies along the length and at $x = 0.5x_0$ it is equal to 0.02, which is a larger value than that obtained from equation (15), i.e. $A = 0.0058$. In Fig. 11, the dashed line shows the trend in the change of the longitudinal temperature gradient at the cross-section $y = 0$ ($A_{y=0}$), and the dashed-dotted line shows a change of $A_{y=+1}$ near the upper bounding surface at $x = 0.5x_0$. It follows from this figure that solutions (15)–(17) are valid at $Ra < 10^5$, and that deviation from solution (15) manifests itself earlier near the bounding horizontal surfaces.

At $Ra = 7.1 \times 10^5$ [Figs. 12(a)–(c)], the flow has the boundary layer pattern. The temperature changes near

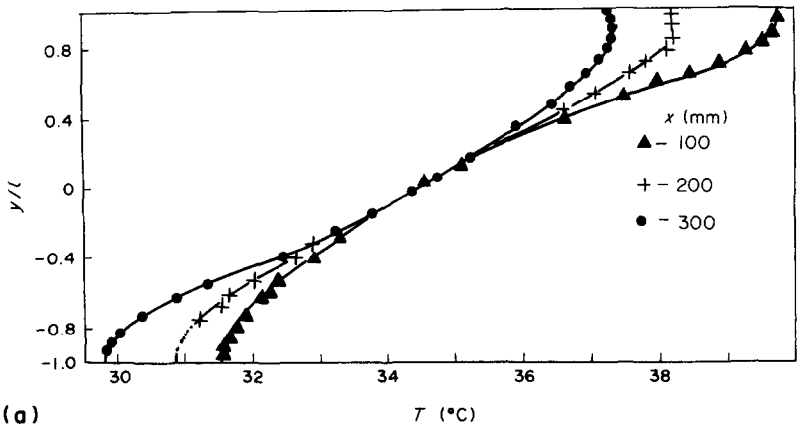

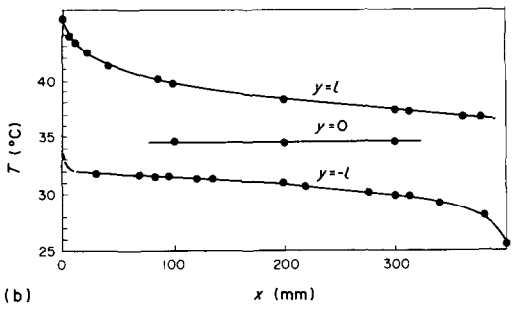

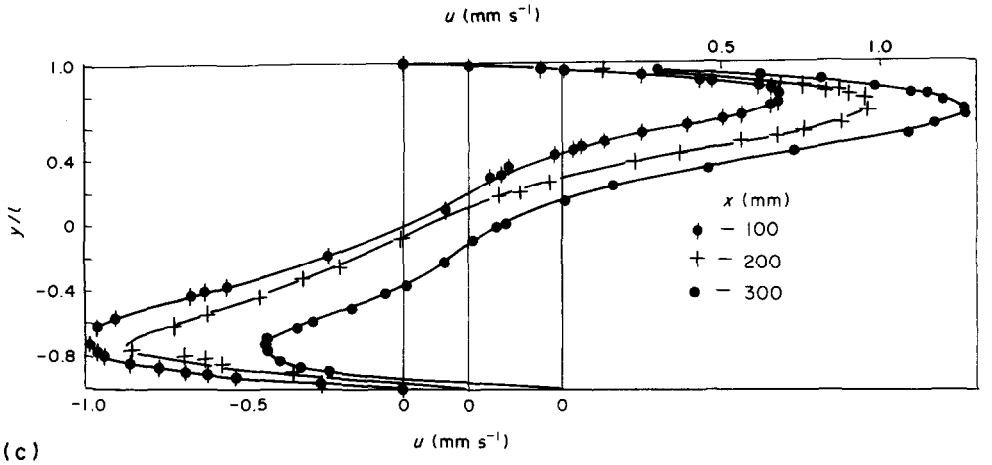

FIG. 12. Temperature profiles over the layer depth at $x = 100$, 200, and 300 mm (a), on the bounding rigid surfaces (b) and velocity profiles (c) at $2l = 29$ mm, $Ra = 7.1 \times 10^5$, $Pr = 4.8$; $x_0 = 412$ mm.

the adiabatic surfaces; $(\partial T/\partial x)_{y=\pm 1}$ is variable along the layer length; the velocity profile differs from the parabolic one [equation (16)]. At $Ra = 6.6 \times 10^6$ [Figs. 13(a)–(c)], the relative thickness of the boundary layer decreases and the zone over y, where $\partial T/\partial y = \text{const.}$ and $\partial T/\partial x = 0$, increases [Figs. 3(a) and (b)]. The flow in the boundary layer becomes more complex: the main stream is localized near the horizontal surfaces and slow counter-currents originate.

At $Ra = 5 \times 10^7$ [Figs. 14(a) and (b)], the velocity profile is still more complex; the thickness of the thermal and velocity boundary layers amounts to 15% of the layer thickness. A stratified flow is observed [Fig. 14(a)]. The region, where $\partial t/\partial y = \text{const.}$ and $\partial T/\partial x = 0$, comes to 70% of the layer thickness.

In Fig. 15, the points present the experimental values of $Nu = Q/2\lambda\Delta T$ at different values of Ra. The heat fluxes were determined by equation (19) from

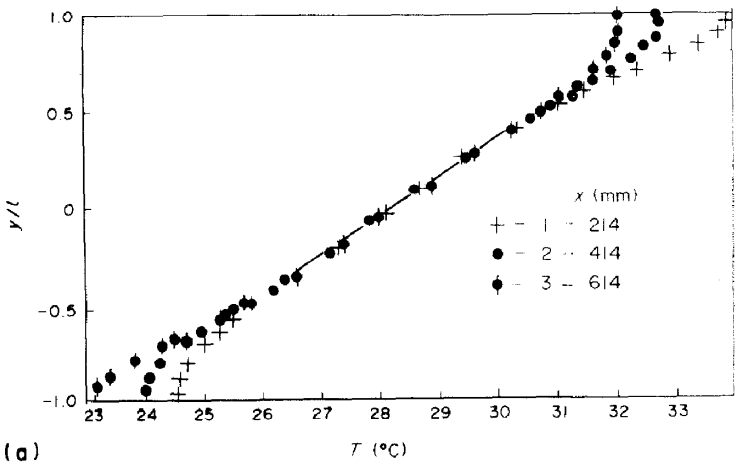

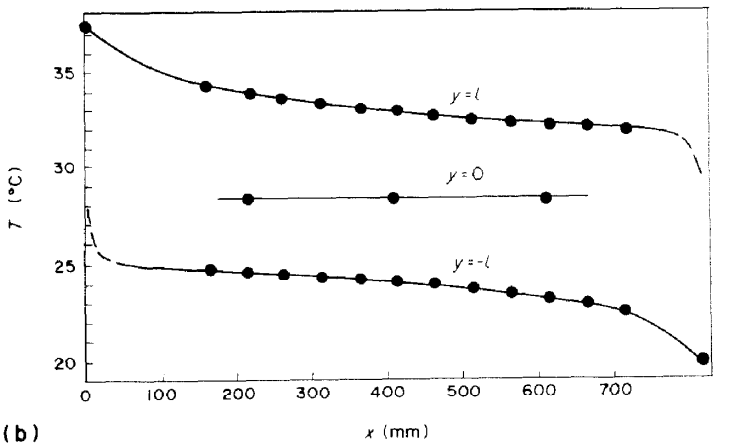

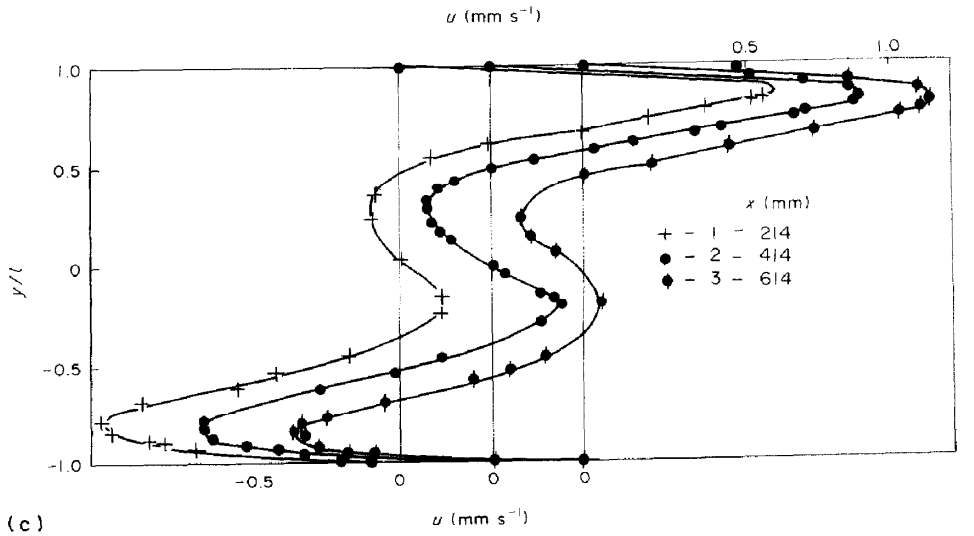

FIG. 13. Temperature profiles over the layer depth at $x = 214$, 414, and 614 mm (a), on the bounding rigid surfaces (b) and velocity profiles (c) at $x = 214$, 414, and 614 mm for the layer $x_0 = 810$ mm, $2l = 64.5$ mm, $Ra = 6.6 \times 10^6$, $Pr = 5.6$.

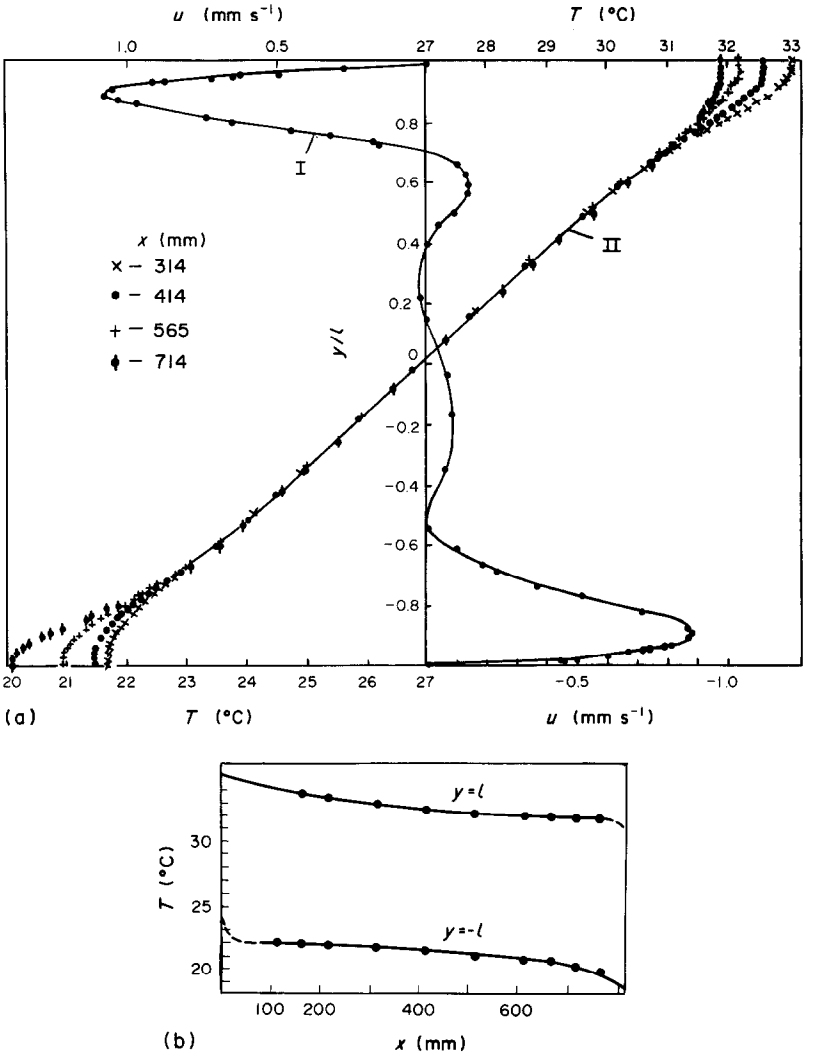

FIG. 14. (a) Profiles of velocity (I) and temperature (II) over the layer depth. (b) Temperature profiles on the bounding rigid surfaces at $x_0 = 810$ mm, $2l = 117.7$ mm, $Ra = 5 \times 10^7$, $Pr = 5.6$.

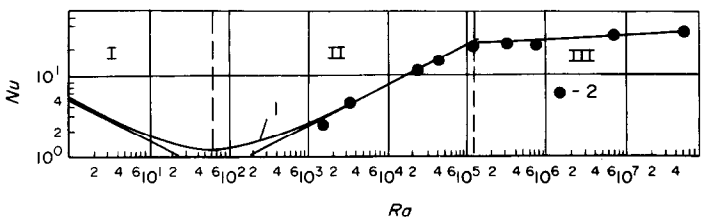

FIG. 15. The dependence of Nu on Ra for the regimes: of heat conduction (I), convection with a plane-parallel flow (II) and of boundary layer (III) for rigid adiabatic horizontal surfaces with heating on one side: 1, equation (21); 2, experimental values, water.

experimental velocity and temperature profiles. At $Ra \ll 63$, the heat conduction regime prevails; at $10^5 > Ra \gg 63$, the regime of the convective heat transfer with a plane-parallel flow in the horizontal layer and at $Ra > 10^5$, the boundary layer regime. In the latter case, a small dependence of Nu on Ra is observed

$$Nu = 12.5Ra^{1/18}. \tag{37}$$

The results of ref. [9] are not presented in Fig. 15, since the experiments were carried out in the conditions of heat transfer through the upper horizontal surface, which is evident from the temperature profiles: the temperature gradient $(\partial T/\partial y)_{y=+l}$ even exceeds $(\partial T/\partial y)_{y=0}$ at the centre of the layer at section $y = 0$. From the initial data available in ref. [9] it is impossible to estimate the quantity of heat transported through the horizontal top plate and that transported horizontally.

At $Pr = 4.5$–5, the stability loss in the plane-parallel flow was not observed, and only its transition into the boundary layer regime was detected. In the boundary layer regime the complication of flow was accompanied by the appearance of horizontal counter-currents over the layer depth; the quantity of strata increased with Ra.

The velocity profile, equation (17), provides the conditions for stable density stratification over the layer core depth. According to ref. [18], at $Ri > 0.0417$ the flow in the boundary layer is always stable where

$$Ri_0 = -g\left(\frac{\partial\rho}{\partial y}\right)_0 \Big/ \rho\left(\frac{\partial u}{\partial y}\right)_0^2 = \beta g\left(\frac{\partial T}{\partial y}\right)_0 \Big/ \left(\frac{\partial u}{\partial y}\right)_0^2,$$

is the Richardson number.

As it follows from equations (16) and (17), for a horizontal layer $Ri_0 = \frac{3}{2} Pr$ at the section $y = 0$, i.e. Ri_0 decreases linearly with Pr and may be as small as one pleases. (In crystal growing technology, liquids are known with $Pr < 10^{-2}$.) The velocity profile, equation (16), has the inflexion point at $y = 0$ and is potentially unstable [2, 3], therefore this flow can be unstable at $Pr \ll 1$.

CONCLUSION

The main attention in the present work was paid to the flow structure in a horizontal layer with adiabatic walls in that portion of it, where the effect of end region flows becomes degenerate. In this case, the main initial parameters are the layer height and the heat flux (or the temperature drop between the adiabatic surfaces). Depending on the determining criterion Ra, based on l and ΔT, the boundaries of the following regimes have been found: of heat conduction, convective heat transfer under the conditions of plane-parallel flow and of the boundary layer. The heat transfer laws have been established. In the latter case, the heat transfer law has been determined for $Pr = 4.5$–5.5 and $x_0/2l = 7$–14.

The laws governing the velocity and temperature field variation in the layer at $\partial T/\partial x = \text{const}$. have been determined analytically under the conditions of thermogravitational convection for two rigid surfaces and under the conditions of simultaneous effect of thermogravitational and thermocapillary forces, with the upper surface being free.

It is shown that in the boundary layer regime, $\partial T/\partial y = \text{const}$. and $\partial T/\partial x = 0$ over the greater portion of the horizontal layer, except for the region near the walls. This points to the possibility for the formation of a linear temperature gradient in pools with side heating when the vertical surfaces are cooled and the free upper and rigid lower bounding horizontal surfaces are insulated.

For the problem considered at the prescribed temperature difference on the vertical end faces of the layer, the determining parameters are

$$Ra_1 = \beta g \Delta T_1 l^3/av; \quad Pr = v/a; \quad x_0/2l.$$

Different combinations of the heat transfer regimes near the vertical surface and in the horizontal layer are possible [Figs. 16 (a) and (b)]

The vertical end surface	Horizontal layer
Regimes	
Heat conduction ($A = \text{const.}$)	Plane-parallel flow ($A = \text{const.}$)
Boundary layer	Plane-parallel flow ($A = \text{const.}$)
Laminar boundary layer	Boundary layer
Transitional from laminar to turbulent	Boundary layer
Turbulent boundary layer	Boundary layer

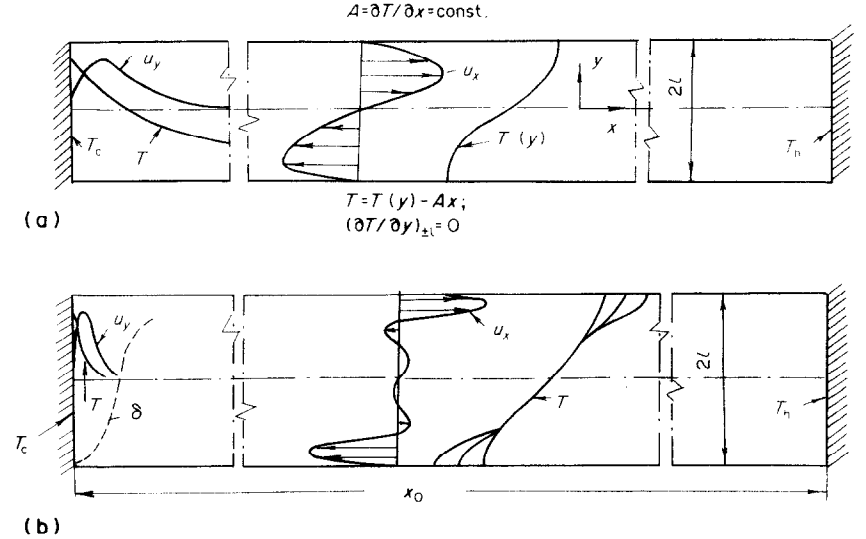

FIG. 16. Schematic diagram of flow near the vertical end surfaces and in the layer core with a plane-parallel flow (a) and in the boundary layer regime near the horizontal surfaces (b).

In solving this multiparametric problem, it is useful to combine the laboratory and numerical experiment with the analytical approximate methods of investigations [13, 14].

REFERENCES

1. R. V. Birikh, On thermocapillary convection in a horizontal layer of liquid, *Prikl. Mat. Tekh. Fiz.* No. 3, 67–72 (1966).
2. G. Z. Gershuni, E. M. Zhukhovitsky and V. M. Myznikov, About the stability of a plane-parallel convective liquid flow in a horizontal layer, *Prikl. Mat. Tekh. Fiz.* No. 1, 95–100 (1974).
3. G. Z. Gershuni, E. M. Zhukhovitsky and V. M. Myznikov, The stability of a plane-parallel convective liquid flow in a horizontal layer against spatial perturbations, *Prikl. Mat. Tekh. Fiz.* No. 5, 145–147 (1975).
4. V. M. Myznikov, On the stability of stationary adequate liquid motion in a plane horizontal layer with a free boundary, in *Convective Flows*, pp. 52–57. Perm (1979).
5. V. M. Myznikov, On the stability of stationary adequate motion in a horizontal layer with a free boundary against spatial perturbations, in *Convective Flows*, pp. 76–82. Perm (1981).
6. V. M. Myznikov, The finite-amplitude spatial perturbations of the adequate motion in a horizontal layer with a free boundary, in *Convective Flows*, pp. 83–88. Perm (1981).
7. J. E. Hart, Stability of thin non-rotating Hadley circulations, *J. Atmos. Sci.* **28**, 687–697 (1972).
8. J. Imberger, Natural convection in a shallow cavity with differentially heated end walls, Part 3. Experimental results, *J. Fluid Mech.* **65**(2), 247–260 (1974).
9. A. Bejan, A. A. Al-Homoud and J. Imberger, Experimental study of high-Rayleigh-number convection in a horizontal cavity with different end temperatures, *J. Fluid Mech.* **109**, 283–299 (1981).
10. G. Z. Gershuni, E. M. Zhukhovitsky and E. A. Tarunin, Numerical investigation of the stationary convection in a cavity of rectangular cross-section with a free upper boundary, *Uch. Zap. Perm. Univ.* No. 248, *Gidrodinamika* No. 3, 106–124 (1971).
11. D. E. Cormack, L. G. Leal and J. H. Seineeld, Natural convection in a shallow cavity with differentially heated end walls, Part 2. Numerical solutions, *J. Fluid Mech.* **65**(2), 231–246 (1974).
12. G. Shiralkar, A. Gadgil and C. L. Tien, High Rayleigh-number convection in shallow enclosures with different end temperatures, *Int. J. Heat Mass Transfer* **24**, 1621–1629 (1981).
13. D. E. Cormack, L. G. Leal and J. Imberger, Natural convection in a shallow cavity with differentially heated walls, Part 1. Asymptotic theory, *J. Fluid Mech.* **65**(2), 209–229 (1974).
14. A. Bejan and C. L. Tien, Laminar natural convection heat transfer in a horizontal cavity with different end temperatures, *Trans. Am. Soc. Mech. Engrs*, Series C, *J. Heat Transfer* **100**(4), 87–94 (1978).
15. P. G. Simpkins and T. D. Dudderas, Convection in rectangular cavities with differentially heated end walls, *Fluid Mech.* **110**, 433–456 (1981).
16. A. G. Kirdyashkin, The structure of thermal gravitational and thermocapillary flows in a horizontal layer of liquid under the conditions of a horizontal temperature gradient, Preprint No. 79–82, Institute of Thermal Physics (1982).
17. N. B. Vargaftik, *Handbook of Thermophysical Properties of Gases and Liquids* (2nd revised and augmented edn.). Izd. Nauka, Moscow (1972).
18. G. Schlichting, *Grenzschicht-Theorie*, Verlag G. Braun, Karlsruhe (1965).

ECOULEMENTS THERMOGRAVITATIONNELS ET THERMOCAPILLAIRES DANS UNE COUCHE LIQUIDE HORIZONTALE SOUS LES CONDITIONS D'UN GRADIENT DE TEMPERATURE HORIZONTAL

Résumé—On présente une étude expérimentale des structures thermiques et dynamiques des écoulements thermogravitationnels dans une couche horizontale chauffée par le côté et ayant deux frontières rigides. La surface supérieure de la couche est libre et celle inférieure est rigide et adiabatique. Ceci crée une situation favorable à la simultanéité de forces thermogravitationnelles et thermocapillaires. Les frontières des régimes thermiques sont déterminées et pour chacune des lois de transfert thermique sont précisées. Pour le régime caractérisé par un gradient longitudinal de température constant (loin des surfaces verticales), les lois gouvernant les champs de vitesse et de température qui dépendent du flux de chaleur sont trouvées analytiquement.

THERMOGRAVITATIONS- UND THERMOKAPILLARSTRÖMUNGEN IN EINER HORIZONTALEN FLÜSSIGKEITSSCHICHT AUFGRUND EINES HORIZONTALEN TEMPERATURGRADIENTEN

Zusammenfassung—Es wird über eine experimentelle Untersuchung der thermischen und dynamischen Struktur von Thermogravitationsströmungen in einer horizontalen, von der Seite beheizten Schicht mit zwei festen Berandungen berichtet. Die obere Grenze der Schicht ist eine freie Oberfläche, die untere fest und adiabat. Diese Anordnung führt zum gleichzeitigen Auftreten von Thermogravitations- und Thermokapillarkräften. Die Grenzen einzelner Wärmeübergangsbereiche wurden gefunden und für jeden Bereich die entsprechenden Wärmeübergangsgesetze aufgestellt. Für den durch einen konstanten Temperaturgradienten in Längsrichtung gekennzeichneten Bereich (weit entfernt von den vertikalen Endflächen), wurden die maßgebenden Gesetze für die Veränderung des Geschwindigkeits- und Temperaturfeldes in Abhängigkeit von der Wärmestromdichte gefunden.

ТЕПЛОВЫЕ ГРАВИТАЦИОННЫЕ И ТЕРМОКАПИЛЛЯРНЫЕ ТЕЧЕНИЯ В ГОРИЗОНТАЛЬНОМ СЛОЕ ЖИДКОСТИ В УСЛОВИЯХ ГОРИЗОНТАЛЬНОГО ГРАДИЕНТА ТЕМПЕРАТУРЫ

Аннотация—Экспериментально исследуется тепловая и динамическая структура тепловых гравитационных течений в горизонтальном слое, подогреваемом сбоку, с двумя жесткими границами, а также с верхней свободной и нижней жесткой адиабатическими поверхностями. В последнем случае наблюдается совместное действие термогравитационных и термокапиллярных сил. Найдены границы режимов теплообмена и для каждого режима определены законы теплообмена. Для режима, характеризуемого постоянным продольным градиентом температуры (вдали от вертикальных торцов) аналитически найдены закономерности изменения поля скорости и температуры в зависимости от теплового потока.